

Calculating the Solvent Exposed Surface Area of Proteins with Intersecting Spheres

Gargi Kher, Neil Gupta

June 8, 2020

Contents

1	Abstract	2
2	Previous Work	2
2.1	Geometrical Representation of Atoms	2
2.2	The Shrake-Rupley Algorithm	3
2.3	Richmond's Algorithm and the Gauss-Bonnet Theorem	4
3	The Power Diagram Model	5
3.1	Model Assumptions	5
3.2	Power Diagrams	5
3.3	Application to Protein Structures	6
3.4	Direction Preserving Motion	9
3.5	Distance Preserving Motion	11
3.6	Combining the Area Equations	13
4	Application of ALPHAMOL to Molecular Modeling	14
5	Conclusion	14
6	Glossary	16
7	Supplemental Information	16
8	References	19
	List of Figures	19

1 Abstract

Calculating the solvent-exposed surface area (SASA) of large biomolecules is an important problem in structural biology, especially in the case of proteins, where small changes in the molecule's shape can greatly limit the protein's ability to do its job. The fraction of a polar atom's surface area that is exposed to the engulfing solvent can be the difference between a stable hydrogen bond being formed with the solvent and a polar atom buried within the protein, which could prevent the protein from folding into its proper shape. Molecular dynamics simulations, which use computers to predict the time evolution of a molecular system also rely on accurate SASA calculations as a way to compute the enthalpy of hydration for the molecules in the system. Today, SASA is usually calculated based on an implicit solvation model, where the solvent is taken to be a continuous field that the molecules of interest sit in. The atoms are taken to be spheres of definite radius, and thus calculating the SASA of an atom involves calculating the fraction of the sphere that is exposed. The SASA of the entire molecule can be found by summing this quantity over all atoms. This paper gives an overview of ALPHAMOL, a way of analytically calculating the derivative of SASA with respect to time, a quantity which can be numerically integrated as part of a molecular dynamics simulation to predict the future state of a molecular system. The chief benefits over other algorithms are numerical stability and an ability to consider internal atoms, which older SASA calculators sometimes ignored.[1] We also discuss two previous ways of computing SASA that ALPHAMOL improves upon. Finally we do some calculations of our own to benchmark the performance of these two methods and provide some modern context for where SASA computations are used.

2 Previous Work

Accurately and quickly calculating the SASA of proteins has been a problem that people have been trying to solve since the 1980's. One reason for this is the fact that the effective potential for solvation can be written $W = W_{elec} + W_{np}$, where W_{elec} represents the electrostatic contribution and W_{np} represents the nonpolar contribution to this potential. The second term depends heavily on the SASA value of the polar atoms in the molecule, as polar atoms with a low SASA value (buried polars) should to make internal hydrogen bonds to preserve the protein's structure. One of the earliest ways of computing this value was by Richmond (1984). His method involved modeling atoms as spheres and computing SASA as an application of the Gauss-Bonnet Theorem. This method was the basis for many future SASA calculators that optimized for attributes like speed or numerical stability. Other methods didn't focus as much on exact values in the interest of speed. The Shrake-Rupley algorithm (optimized by Legrand and Merz as discussed below), breaks up the spherical surface of each atom into a set of dots, and uses the fraction of dots that are exposed as a proxy for the exposed surface area. This is the default SASA calculator in Rosetta, a software package developed at the UW that allows for the computational analysis and design of protein structures.

2.1 Geometrical Representation of Atoms

While atoms are comprised of protons, neutrons, and electrons, electrons are what give them their properties. Electrons make up the volume of an atom, and are generally found near the nucleus. Because we don't know for certain where electrons are in an atom, their positions are represented by orbitals, which give the probability of electrons being in a particular location. Orbitals can take

on different shapes, generally resembling some type of dumbbell, but when they come together, they form a roughly spherical shape (DeCoste, Zumdahl p.551-557). This is why atoms are often mathematically modeled as spherical objects.

2.2 The Shrake-Rupley Algorithm

The Shrake-Rupley Algorithm (Shrake and Rupley, 1973) is the standard way of calculating SASA by approximating the surface as a discrete set of voxels instead of a continuous surface. This can lead to inaccuracies, but the gains in speed are usually worth it. The algorithm can also fail if the protein surface is not continuous (i.e. an internal cavity is present) or the atomic radii are too small. This algorithm, once optimized by Legrand and Merz (1993) became a standard SASA calculator. Comparing this algorithm with the analytic SASA calculator MSEED (Perrot et al.) in calculating the SASA of the protein BPTI showed Shrake-Rupley to be roughly six times faster than MSEED, a huge improvement. The method works by representing the surface of sphere a_i by an array of l points evenly distributed on the surface of a sphere of radius r_i . The exposed surface area of a_i can be written as

$$A_i = 4\pi r_i^2 \frac{l_{exposed}}{l_{total}} \quad (1)$$

where $l_{exposed}$ is the number of points that are solvent exposed. Now if we were to calculate this quantity for each atom we would need to make nkl calculations, where k is the average number of atoms that intersect a given atom. This could get quite intensive. What Legrand and Merz did was realize that any surface point is either buried or exposed, and thus the state of a_i 's surface points could be represented as an $l/8$ byte string b_i , where $b_{ij} = 1$ means that the point is exposed and $b_{ij} = 0$ means that the point is buried. This has the benefit of making the calculation of the points on a_i buried by a neighboring sphere a_q a boolean AND operation on b_i . By defining m_{iq} as a boolean string with k^{th} element 0 when the k^{th} point of sphere a_i is buried by a_q and 1 otherwise, the set of points on a_i left exposed by the intersection with a_q is $(111...1) \& m_{iq}$. Thus

$$b_i = (111...1) \& m_{i1} \& m_{i2} \& m_{i3} \& \dots \& m_{ik} \& m_{ik+1}$$

for each a_k that intersects a_i . The SASA of a_i can then be calculated by (1) by setting $l_{exposed}$ as the number of bits in b_i .

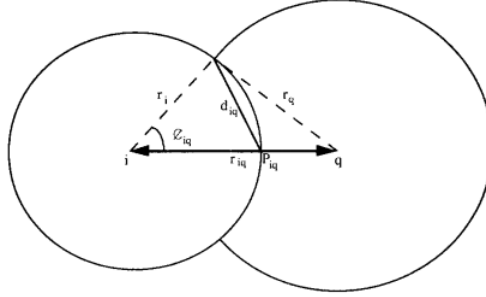
To actually calculate m_{iq} , we first compute

$$\cos \theta_{iq} = \frac{r_i^2 + r_{iq}^2 - r_q^2}{2r_i r_{iq}} \quad (2)$$

$$d_{iq} = 2r_i \sin \theta_{iq} = 2r_i \sqrt{\frac{1 - \cos \theta_{iq}}{2}} = r_i \sqrt{2(1 - \cos \theta_{iq})} \quad (3)$$

All points on a_i within d_i of the P_{iq} are buried, and those bits in m_{iq} are set to zero, with the rest set to 1. This string can be AND'ed with b_i to produce a new b_i . This can be done for all spheres that intersect a_i for each sphere in turn. The key insight that cuts down on the nkl calculations is the fact that the m_{iq} can be stored and retrieved later if the same string is ever needed. This is very likely to occur, because the d_{iq} can be made independent of r_i by removing the factor r_i . Then $d_{iq} = \sqrt{2(1 - \cos \theta_{iq})}$. Now we can calculate m_{iq} for the range of d_{iq} from 0-2. Once we store these masks, we will have covered all possible overlaps between spheres because we have gone through all

Figure 1: Calculation of d_{iq} and θ_{iq} for the purpose of calculating m_{iq} .



angles θ_{iq} . This provides a method of calculating the SASA of the entire protein. We can simply look at every intersection with a given atom and lookup the appropriate mask (based on the angle θ_{iq}). Then we scale it by the radius of the atom we are looking at. Then we can perform our AND operations and find the SASA for a given atom. Iterating over all atoms gives us our answer.

A possible way to improve this method is to increase the number of dots on each atom l . Of course, in doing this you trade off time for accuracy. However that tradeoff is a fundamental one in numerically solving almost modeling problem.

2.3 Richmond's Algorithm and the Gauss-Bonnet Theorem

In a previous paper written by Richmond (1984), a different strategy is used to find the solvent exposed surface area of the atoms. He still represents the atoms as spheres with definite radius with centers at the atomic coordinates, but instead of using voxels, he made use of the Gauss-Bonnet theorem, a fundamental theorem in differential geometry which connects the topological properties of a manifold (specifically its Euler Characteristic) with its geometric properties (its curvature). A standard statement of the theorem is

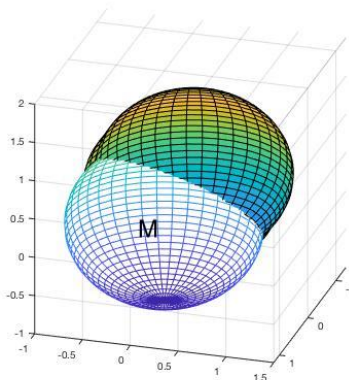
$$\int_M K dA + \int_{\partial M} k_g ds = 2\pi\chi(M) \quad (4)$$

Here χ is the Euler Characteristic of M , and K and k_g are the Gaussian and geodesic curvatures of the manifold and the boundary respectively. For polygons, $\chi = V - E + F = 1$.

The SASA of an atom with radius ρ_i lies on a sphere where $K = \frac{1}{\rho_i^2}$. We can divide this SASA into many polygons bounded by the circles of intersection with neighboring spheres (See Figure 2). If M is one particular region of that SASA, we can write

$$\begin{aligned} \frac{1}{\rho_i^2} \int_M dA + \int_{\partial M} k_g ds &= 2\pi \\ \implies A &= \rho_i^2 \left(2\pi - \int_{\partial M} k_g ds \right) \end{aligned} \quad (5)$$

Figure 2: Two Intersecting Spheres



Thus if we know k_g (the geodesic curvature) of the boundary of M at all points, we can compute A . If ∂M is piecewise smooth, then $\int_{\partial M} k_g ds$ is the sum of the integrals along the components of the boundary plus the sum of the angles by which the elements of the boundary turn at the corners. For the simple example of a geodesic triangle on a sphere of radius ρ , $\int_{\gamma} k_g ds = 0$ where γ is a piece of ∂M . Thus $\int_{\partial M} k_g ds = 0 + \sum (\pi - \alpha_i)$, where α_i are the interior angles of the triangle. Plugging this into (5) gives $A = \rho^2(-\pi + \sum \alpha_i)$. This is the well known Girard's Theorem.

In our case, the boundaries of M won't be piecewise geodesic, and thus calculating $\int_{\partial M} k_g ds$ will require knowledge of the circles of intersection between the spheres. With that data calculating k_g simply requires some vector calculus. We can calculate the SASA of the entire protein this way, by adding up the contributions of the individual regions M across all atoms.

3 The Power Diagram Model

3.1 Model Assumptions

As has already been explained and will be mentioned later on, one of the biggest assumptions made by this model is by representing each atom as a ball. This ball is surrounded by a sphere whose distance from the edge of the ball represents the radius of a solvent sphere (Figure 3). A solvent refers to a liquid the molecule is suspended in, usually water. This solvent is being represented continuously rather than as a collection of atoms.

3.2 Power Diagrams

Our protein can be represented as a set of atom centers S in \mathbb{R}^3 with their corresponding balls of various radii. One aspect of the model is computing the power diagram of this protein. The power diagram is a generalized Voronoi diagram, where instead of the normal Euclidean metric, the definition for distance between an atom with center z_i and radius ρ_i and a point x is $\pi_i(x) = \|x - z_i\|^2 - \rho_i^2$. This becomes the default Voronoi diagram of S if all the radii are equal. After this

power diagram is generated we can associate each set of atoms S_i with its corresponding power cell P_i defined by

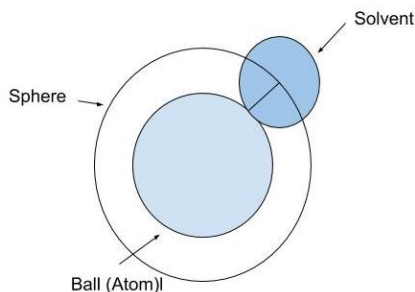
$$P_i = \{x \in \mathbb{R}^3 \mid \pi_i(x) \leq \pi_j(x), \forall j\}$$

Each P_i is convex, and together they cover all \mathbb{R}^3 without overlap. The dual of this power diagram, or alpha shape, is a weighted Delaunay Triangulation of S into a set of simplices, or triangles and tetrahedrons. We can compute the surface area of these balls using Delaunay triangulation, which will help us in the later sections. There are additional rules for constructing Delaunay triangles, but for the purposes of this paper, it is only necessary to know how they are constructed from the atoms.

3.3 Application to Protein Structures

Consider a set of balls B_i defined by a center z_i and a fixed radius ρ_i to be our protein. To represent the entire state of the protein (with n atoms) we use the $m = 3n$ dimensional vector $\mathbf{z} \in \mathbb{R}^{3n}$ where $[\mathbf{z}_{3i+1}, \mathbf{z}_{3i+2}, \mathbf{z}_{3i+3}]^T = z_i$. Note that $0 \leq i \leq n-1$. Now we can define the weighted and unweighted surface areas $E, A : \mathbb{R}^{3m} \rightarrow \mathbb{R}$ as real multivariate functions from the state of the protein to a single value (the solvent exposed surface area). The weighted area will be described below. Here we will describe the gradients of these maps, written as $DE_{\mathbf{z}}$ and $DA_{\mathbf{z}}$ which would allow us to calculate SASAs for protein structures and approximate how the SASA changes as the atomic coordinates move. These derivatives map each point in \mathbb{R}^m to a corresponding gradient vector that we call \mathbf{u} .

Figure 3: B_1 is bound by a sphere. We can think of the sphere as how much of the solvent can interact with the atom.



Given a collection of atoms, there will be many overlapping spheres in \mathbb{R}^{3n} . We will describe area derivative equations for groups of two or three overlapping spheres, which can easily be applied to larger systems. Using the power method described above, we will show how the authors use Delaunay Triangulations to assist with the calculations.

In order to derive the SASA equations, we must define some additional terms. After constructing Delaunay Triangles from a set of molecules, the “star” and “link” of the alpha shape’s subcomplex are defined. Each of the Delaunay triangles is a simplex. K is defined as a dual complex, or subcomplex of the alpha shape.

Figure 4: Three balls in space bounded by three different spheres. Their centers are used for Delaunay Triangulation.

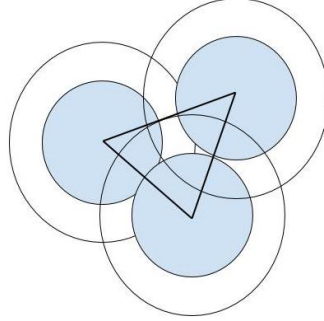


Figure 5: A power diagram comprised of power cells (left) and its Delaunay Triangulation (right).[1]

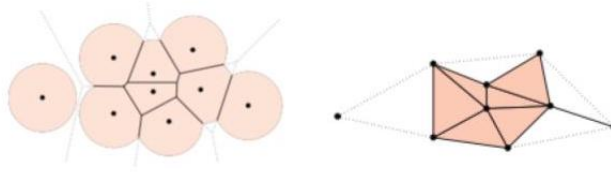
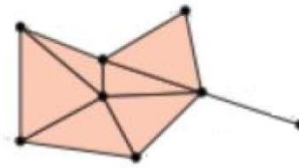


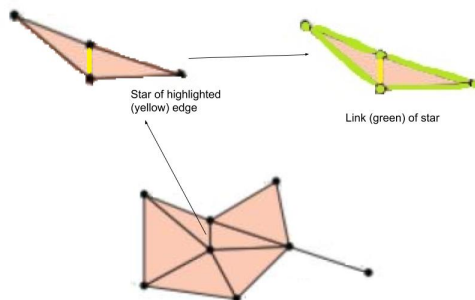
Figure 6: The dual complex (K) of the Delaunay Triangulation only includes those power cells that have a non-empty intersection.[1]



As can be seen by Figure 6, K is made up of multiple simplices. The star of K is a set of triangles who share a vertex and outside boundary. The link of K , then, is all of the vertices and edges in

the star (Figure 7).

Figure 7: The star of K and link of the star are shown.[1]



Knowing how the star and link of a subcomplex K are defined is useful when deriving the SASA equations. The collection of spheres, or the entire molecule, is known as a space-filling diagram F . F_i , for instance, consists of all the atoms in S_i . σ represents the fraction of a sphere on the boundary of F . We only really care about the boundary of F because that is what contributes to the exposed surface area that will be interacting with the solvent. As mentioned earlier, a molecule can contain multiple spheres that overlap. For two intersecting spheres S_i and S_j that share a circle S_{ij} , σ comes out to:

$$\sigma_{ij} = \frac{\text{length}(P_i \cap P_j \cap \text{bd}F)}{\text{length}(S_{ij})} \quad (6)$$

$\text{bd } F$ means the boundary of F . This equation shows that for the space-filling diagram of the two intersecting spheres, σ_{ij} is the fraction of the exposed surface that's on the power cells of both of the spheres. Using the dual complex, we can further specify the equation for σ_{ij} in terms of two intersecting circles, which will become useful later:

$$\sigma_{ij} = 1 - \frac{\sum_k \text{length}(S_{ij}^k) - \sum_{k,l} \text{length}(S_{ij}^k \cap S_{ij}^l)}{2\pi \varrho_{ij}} \quad (7)$$

This equation is derived by looking at Edelsbrunner's (1995) paper. The same two spheres S_i and S_j intersect at S_{ij} . However this time, S_{ij}^k and S_{ij}^l are the intersection of S_{ij} with two other spheres (S_k and S_l) in the power diagram. Both S_{ij}^k and S_{ij}^l minimize the power distance to S_{ij} . Looking at the right side term of equation 7, the first sum adds the portion of S_{ij} coming into contact with S_k , while the second sum adds the portion of S_{ij} coming into contact with both S_k and S_l . Having this second sum ensures we don't over count the amount of unexposed area. Dividing the difference of these sums by the circumference of the circle gives the fraction of this unexposed area, so that subtracting this term from 1 gives the fraction of the exposed surface area of F .

σ is related to the area of the ball, which for a ball with radius ϱ is $4\pi\varrho^2$. Because we only care about the exposed surface area, we need to multiply by σ , in order to only get the solvent-exposed surface area. We can also define a weighted area, which only differs from the unweighted area equation by the factor of some parameter α , which represents some constant atomic solvation parameters that were predefined by Eisenberg and McLachlan (1986). So for just one ball B_i :

$$A = 4\pi \sum \varrho_i^2 \sigma_i \qquad E = 4\pi \sum \alpha_i \varrho_i^2 \sigma_i$$

Another term, β_{ijk} , is also used, which is useful when considering the case of three intersecting spheres. When three spheres intersect at two points, there is a line segment passing through them that is represented as B_{ijk} . Just like for σ_{ij} , β_{ijk} represents the fraction of points that belong to the edge of F for these three spheres.

$$\beta_{ijk} = \frac{\text{length}(P_i \cap P_j \cap P_k \cap \text{bd}F)}{\text{length}(B_{ijk})} \quad (8)$$

A similar expression to σ_{ij} is derived for β_{ijk} , using B_{ijk}^l , the portion of the line segment B_{ijk} on a fourth sphere S_l .

$$\beta_{ijk} = 1 - \frac{\sum_l \text{length}(B_{ijk}^l)}{\text{length}(B_{ijk})} \quad (9)$$

In the right side term of equation 9, the sum adds up the length of the line segment that comes in contact with S_l and divides that by the entire length of B_{ijk} (which is $2\varrho_{ijk}$), giving the fraction of F that is unexposed. By subtracting this term from 1, the fraction of solvent exposed area for the three intersecting spheres is found.

Because the area derivatives are linear, they can be broken down into a sum of components. Both unweighted and weighted area derivatives are comprised of two motions, direction preserving and distance preserving, which can be derived separately and summed to get the SASA derivatives.

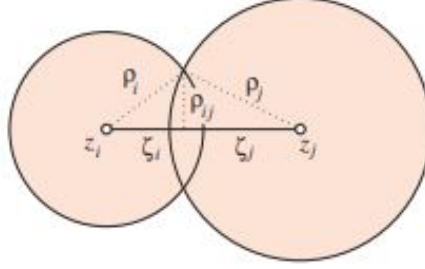
3.4 Direction Preserving Motion

In direction preserving motion, it is assumed that two spheres S_i and S_j bounded with a non-empty intersection are moving straight on the line passing through their centers. In this case, the space-filling diagram F consists of all the atoms in S_i and S_j , in other words $F = B_i \cup B_j$ (Figure 8).

A term ζ_{ij} is equal to $\zeta_i + \zeta_j$, or the norm of the distance between the centers of the two spheres z_i and z_j . ζ in this case represents the signed distance of each sphere center to the circle of intersection. Each of the sphere's own radii are defined to be ρ_i and ρ_j . First, we can assume coordinates for the spheres based on what we know about their centers. $(0,0,z_i)$ can represent the center of S_i and $(0,0,z_j)$ the center of S_j .

The general equation of a sphere ($x^2 + y^2 + z^2 = r^2$) can be used to construct equations for S_i and

Figure 8: Two intersecting spheres S_i and S_j . [1]



S_j :

$$x^2 + y^2 + (z - z_i)^2 = \zeta_i^2$$

$$x^2 + y^2 + (z - z_j)^2 = \zeta_j^2$$

Now we can combine the equations:

$$\zeta_i^2 - \zeta_j^2 = (z - z_i)^2 - (z - z_j)^2 = -2z_i + 2z_j + z_i^2 - z_j^2$$

$$\implies -2z_i + 2z_j + z_i^2 - z_j^2 = (\zeta_i)^2 - (\zeta_j)^2$$

Using this logic, we can find the same equation holds true if we consider the set of balls for each sphere (assuming they have the same radii), as they have the same center as the spheres. So:

$$-2z_i + 2z_j + z_i^2 - z_j^2 = \varrho_i^2 - \varrho_j^2$$

From the above two expressions, we can state that:

$$\zeta_i^2 - \zeta_j^2 = \varrho_i^2 - \varrho_j^2$$

In the left term, we can factor out $\zeta_i^2 - \zeta_j^2$ to get:

$$\zeta_i^2 - \zeta_j^2 = (\zeta_i - \zeta_j)(\zeta_i + \zeta_j) = \zeta_{ij}(\zeta_i - \zeta_j)$$

So we can state that:

$$\varrho_i^2 - \varrho_j^2 = \zeta_{ij}(\zeta_i - \zeta_j)$$

Now we can find what ζ_i and ζ_j really are

$$(\varrho_i^2 - \varrho_j^2)/\zeta_{ij} + \zeta_j = \zeta_i$$

We know that $\zeta_j = \zeta_{ij} - \zeta_i$, so just substitute this expression in:

$$\zeta_i = \frac{1}{2} \left[\zeta_{ij} + \frac{\varrho_i^2 - \varrho_j^2}{\zeta_{ij}} \right]$$

A similar statement can be made for ζ_j , following the steps we carried out above:

$$\zeta_j = \frac{1}{2} \left[\zeta_{ij} + \frac{\varrho_j^2 - \varrho_i^2}{\zeta_{ij}} \right]$$

Now we can find the area of both spheres. For two spheres, it makes sense that $A = A_i + A_j$. Recall the area equation stated in Section 3.3. For two balls we can say: $A = 4\pi \sum \varrho_i^2 \sigma_i + 4\pi \sum \varrho_j^2 \sigma_j$. We have already shown what σ is, so we can plug it in and simplify the area equation:

$$4\pi\varrho_i^2 \frac{\varrho_i + \zeta_i}{2\varrho_i} + 4\pi\varrho_j^2 \frac{\varrho_j + \zeta_j}{2\varrho_j}$$

After a few algebraic simplifications:

$$2\pi\varrho_i^2 + 2\pi\varrho_j^2 + \pi\varrho_i \left(\zeta_{ij} + \frac{\varrho_i^2 - \varrho_j^2}{\zeta_{ij}} \right) + \pi\varrho_j \left(\zeta_{ij} + \frac{\varrho_j^2 - \varrho_i^2}{\zeta_{ij}} \right)$$

$$A = 2\pi(\varrho_i^2 + \varrho_j^2) + \pi(\varrho_i + \varrho_j) \left[\zeta_{ij} + \frac{(\varrho_i - \varrho_j)^2}{\zeta_{ij}} \right]$$

Finally, we can find the derivative of the area with respect to ζ_{ij} :

$$\frac{dA}{d\zeta_{ij}} = \pi(\varrho_i + \varrho_j) \left[1 - \frac{(\varrho_i - \varrho_j)^2}{\zeta_{ij}^2} \right]$$

This is term we get after some simplification.

3.5 Distance Preserving Motion

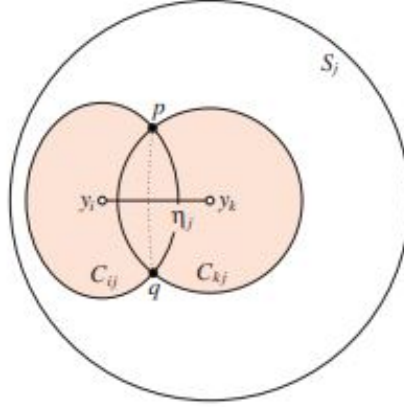
In distance preserving motion, one sphere rotates around the other. Imagine three spheres interesting at two points, p and q (Figure 9). This time, F is going to include all the points contained in all three spheres. It is assumed that if the spheres intersect at two points then one sphere contains the other two. In this case, it is S_j that engulfs S_i and S_k . The caps, or tops of the spheres, are considered. From a previous section, we know that B_{ijk} is considered the line segment of three intersecting spheres. In this case, B_{ijk} is the line segment containing p and q . The caps $C_{ij} = B_i \cap S_j$ and $C_{kj} = B_k \cap S_j$ protrude from the surface of S_j . The parameters obtained from this diagram allows us to find the area similar to how we found it for the direction preserving motion. This model says that as you move the two caps apart, keeping their centers in the same position, you will gain an area equal to that of a spherical rectangle. Essentially, the caps are rotating in place. It might be easy to think about how diameter of the caps can represent the height of this “rectangle” while the distance between the caps signifies its width.

Using this spherical rectangle shape, and the fact that we know the caps are rotating, the change in area for all of the points in both caps is found to be the change in the distance between the center of the caps η_j divided by the circumference of the set of balls in the larger sphere (which is S_j in this case) times the area of the slice of S_j between p and q :

$$dA_j = \frac{d\eta_j}{2\pi\varrho_j} 4\pi\varrho_j\varrho_{ijk}$$

$\frac{d\eta_j}{2\pi\varrho_j}$ takes the change in the distance between the center of the caps over the circumference of B_j . Another way to think about the change in area is seeing $d\eta_j$ as the change in “width” of the spherical rectangle and $2\varrho_{ijk}$ as the length of B_{ijk} , or the height of the rectangle. The area derivative becomes:

Figure 9: Three intersecting spheres at two points: S_i , S_k and S_j . [1]



$$\frac{dA_j}{d\eta_j} = 2\varrho_{ijk}$$

3.6 Combining the Area Equations

Now that we've derived area derivative equations for both types of motions, we can see how they're able to come together. As mentioned before, because the derivatives are linear, they can be separated into a sum of certain components. The gradient vector \mathbf{u} shows the direction or trend of the area. For the case of the direction-preserving motion it is stated $u_{ij} = \frac{z_i - z_j}{\zeta_{ij}}$, showing that the unit vector u_{ij} for two intersecting spheres S_i and S_j is dependent on the distance between their centers. The gradient vector u_{ijk} for distance preserving motion is dependent on the component of the intersection to two of the spheres (u_{ik}) that is normal to the component of intersection between the other two spheres (u_{ij}). This makes $u_{ijk} = \frac{u_{ik} - \langle u_{ik}, u_{ij} \rangle \cdot u_{ij}}{\|(u_{ik} - \langle u_{ik}, u_{ij} \rangle \cdot u_{ij})\|}$.

Based on what has already been shown, the unweighted and weighted area derivative theorems can be stated. Remember that we said each state \mathbf{z} was in \mathbb{R}^{3n} , and each \mathbf{z} represents a set of balls B_i so that $0 \leq i \leq n - 1$. Looking at the area derivative theorem, the derivative of the area at some \mathbf{z} is said to be $DA_z(\mathbf{t}) = \langle \mathbf{a}, \mathbf{t} \rangle$, where \mathbf{a} is a gradient vector like \mathbf{u} and \mathbf{t} is the variable vector mentioned above. They state that for the unweighted area derivative,

$$\mathbf{a} = \sum_j \sigma_{ij} \cdot a_{ij} + \sum_j \sum_k \beta_{ijk} \cdot a_{ijk} \quad (10)$$

The first sum of equation 10 shows the contribution of the direction preserving motion while the second sum shows the contribution of the distance preserving motion. We can see for the first sum that we are summing over all of the points along $\text{bd } F$ in K when considering direction preserving motion for S_i across all S_j . Similarly, the second sum considers distance preserving motion for S_i

across all S_j and S_k in K . From this, a_{ij} and a_{ijk} are:

$$a_{ij} = \pi(\varrho_i + \varrho_j) \left[1 - \frac{(\varrho_i - \varrho_j)^2}{\zeta_{ij}^2} \right] \cdot u_{ij}$$

$$a_{ijk} = 2\varrho_{ijk} \frac{\varrho_i - \varrho_j}{\zeta_{ij}} \cdot u_{ijk}$$

a_{ij} and a_{ijk} depend on the unit vectors u_{ij} and u_{ijk} , respectively.

The weighted area derivative theorem, defined as $DE_z(\mathbf{t}) = \langle \mathbf{e}, \mathbf{t} \rangle$ is defined similarly to the unweighted area derivative theorem, but multiplied by the solvent parameter α :

$$\mathbf{e} = \sum_j \sigma_{ij} \cdot e_{ij} + \sum_j \sum_k \beta_{ijk} \cdot e_{ijk} \quad (11)$$

$$e_{ij} = \pi \left((\alpha_i \varrho_i + \alpha_j \varrho_j) - \frac{(\alpha_i \varrho_i - \alpha_j \varrho_j)(\varrho_i^2 - \varrho_j^2)}{\zeta_{ij}^2} \right) \cdot u_{ij}$$

$$e_{ijk} = 2\varrho_{ijk} \frac{\alpha_i \varrho_i - \alpha_j \varrho_j}{\zeta_{ij}} \cdot u_{ijk}$$

Not surprisingly, e_{ij} and e_{ijk} depend on (respectively) u_{ij} and u_{ijk} as well.

Above, we described \mathbf{a} and \mathbf{e} . Using these, we can then clearly state the area derivative equations. For the unweighted area derivative equation, the direction preserving component is the the fraction of the solvent-exposed surface times the derivative of the area: $\sigma_{ij} < a_{ij}, t_i >$ and the distance preserving component is the same: $\beta_{ijk} < a_{ijk}, t_i >$. We know that the unweighted area derivative is the sum of these two components:

$$DA_z(\mathbf{t}) = \sum_{i=0}^{n-1} \sum_{j \neq i} \left(\sigma_{ij} < a_{ij}, t_i > + \sum_{k \neq i, j} \beta_{ijk} < a_{ijk}, t_i > \right) \quad (12)$$

Just like before, the weighted area derivative is basically the same as the unweighted derivative:

$$DE_z(\mathbf{t}) = \sum_{i=0}^{n-1} \sum_{j \neq i} \left(\sigma_{ij} < e_{ij}, t_i > + \sum_{k \neq i, j} \beta_{ijk} < e_{ijk}, t_i > \right) \quad (13)$$

These are the derivative equations that can then be tested on different molecules. It is important to note that there are cases where these equations will be discontinuous. We won't elaborate on these, but, for example, discontinuities can happen in a case where three spheres intersect at a circle. There are other cases of discontinuities, which will be useful to know in order to successfully run this algorithm for a variety of molecules.

4 Application of ALPHAMOL to Molecular Modeling

To test the time cost of ALPHAMOL (the computational implementation of the method described in §3) versus the Shrake-Rupley Algorithm we took 100 PDB structures from the RCSB[6] database

(listed in the supplemental) with between 30 and 330 residues and directly calculated surface areas using PyRosetta[9], a python wrapper for Rosetta that allowed us to write a script that computed SASA for 100 structures using these two methods. We measured the time to compute SASA for each PDB for each method, and plotted this data against residue count. It can be seen that the ALPHAMOL method is substantially slower than the Shrake-Rupley method and that the time cost of both increases roughly linearly with the size of the structure, though it is clear that ALPHAMOL incurs time penalties faster than Shrake-Rupley as the structure size increases. ALPHAMOL takes roughly $1000 \mu\text{s}$ per residue versus Shrake-Rupley's $200 \mu\text{s}$. The 5x speedup for the latter algorithm makes it an attractive choice for structures without a lot of the internal complexity that makes ALPHAMOL useful.

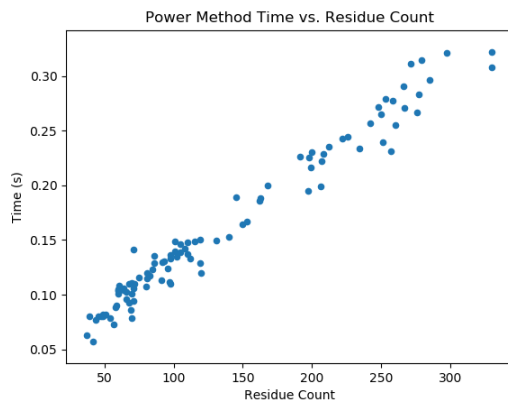


Figure 10: Plot of Computation Time versus Residue Count (Power Method)

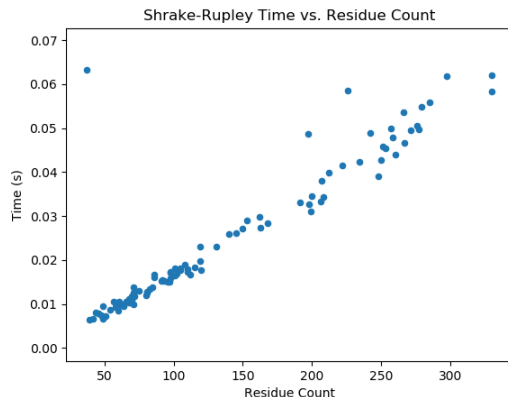
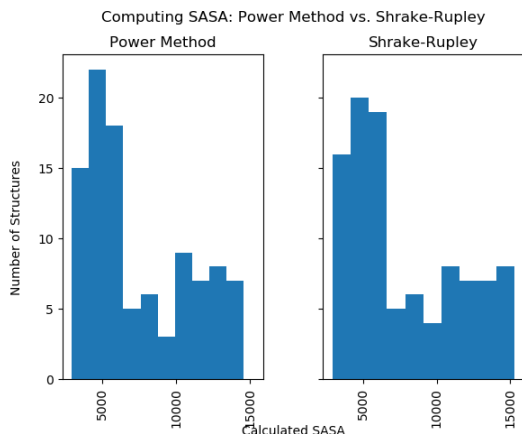


Figure 11: Plot of Computation Time versus Residue Count (Shrake-Rupley Method)

We also plotted the distribution of the SASA values for each calculator, and although they don't look too different in this example, more rigorous testing with a wider range of proteins has shown that

ALPHAMOL gives far more accurate values than other algorithms, chiefly because of its consideration for internal cavities. This is why it is incorporated into Rosetta today.

Figure 12: SASA Histograms for the Two Algorithms



5 Conclusion

It can be seen that SASA is a critical quantity to be able to compute for the purposes of structural biology. On a per-atom basis, it is one metric that can be used to determine if an atom is making a hydrogen bond, and by extension if the structure is energetically favorable. For protein-protein interfaces, large SASA values at the interface usually mean the proteins are more likely to bind because there is a larger binding surface. Metrics like SASA are useful because they don't require your structure to look similar to any existing PDB in order to determine if the structure is likely to be stable. This is especially important in the field of protein engineering, where there might not be any structures to compare your PDB to, and thus having independent metrics is critical to filtering out possible *de novo* protein designs from sequences that won't take on any definite conformation. Thus much time has been spent on applying mathematical and computational ideas to rigorously defining and calculating SASA, and in this paper we have explored a few of the most prominent methods.

6 Glossary

ρ_i :	The radius of ball i
z_i :	The center of a ball i
\mathbf{z} :	The $3n$ dimensional vector representing the state of all z_i
ζ_{ij} :	The signed distance between centers of two intersecting spheres
σ_{ij} :	The fraction of solvent-exposed surface for two intersecting spheres S_i, S_j
β_{ijk} :	The fraction of solvent-exposed surface for three intersecting spheres S_i, S_j, S_k
α :	An atomic solvation parameter
F :	The space filling diagram
$\pi_i(x)$:	The power distance of a random point x from S_i
P_i :	The set of points closer (by power distance) to S_i than any other sphere
K :	The dual complex of Delaunay Triangulation. Consists of all power cells with non-empty intersection
$DA_{\mathbf{z}}(\mathbf{t})$:	The unweighted area derivative at \mathbf{t}
$DE_{\mathbf{z}}(\mathbf{t})$:	The weighted area derivative at \mathbf{t}

7 Supplemental Information

List of PDB's used:

129L, 1A70, 1A7H, 1AHL, 1AIU, 1AVS, 1B3C, 1B4R, 1B7I, 1B7K, 1B7V, 1B8W, 1BB8, 1BCG, 1BF0, 1BMG, 1BWR, 1CDT, 1COU, 1CPZ, 1CRE, 1DC9, 1DZO, 1EMV, 1FGP, 1FI5, 1FRE, 1G47, 1GAJ, 1HA6, 1HA8, 1HYM, 1I2U, 1I9Q, 1IIB, 1IVA, 1KTH, 1L6H, 1NEI, 1P3B, 1QYS, 1RKI, 1RO3, 1S2B, 1SRR, 1THX, 1UBQ, 1VHI, 1W4H, 1WDV, 1WOU, 2ACY, 2APB, 2BCB, 2CA8, 2CBM, 2CM8, 2EBY, 2FD7, 2FLS, 2GNP, 2GQV, 2GZV, 2HSH, 2KXK, 2MCT, 2O35, 2OXZ, 2R32, 2VV9, 2W5L, 2XKH, 2YM4, 2Z9H, 2ZO1, 3CS1, 3PFC, 3PMD, 3RQ8, 3S9B, 3UA6, 4AEI, 4BWS, 4DZN, 4FH1, 4KXO, 4LUP, 4W9A, 4ZK9, 5OH3, 5OIL, 5PC4, 5R2D, 6CQS, 6CW0, 6D40, 6DJA, 6F65, 6G0M, 6MKL.

PyRosetta Code:

```

1 import matplotlib.pyplot as plt
2
3 from pyrosetta import *
4 init("-holes:dalphaball /net/shared/rosetta_builds/bcov_stable/20-04-27-broken/main/
   source/external/DAlpahBall/DAlphaBall.gcc")
5
6 import time
7 import pandas as pd
8 df = pd.DataFrame(columns=['name', 'type', 'sasa'])
9 daltimes = pd.DataFrame(columns=['name', 'Residue Count', 'Time (s)'])
10 voxtimes = pd.DataFrame(columns=['name', 'Residue Count', 'Time (s)'])
11
12 def get_per_atom_sasa_dalpha_ball(pose, probe_size=1.1):

```



```

13     atoms = rosetta.core.id.AtomID_Map_bool_t()
14     atoms.resize(pose.size())
15     for i in range(1, pose.size()+1):
16         atoms.resize( i, pose.residue(i).natoms(), True)
17     surf_vol = rosetta.core.scoring.packing.get_surf_vol( pose, atoms, probe_size)
18     return surf_vol
19
20 def get_per_atom_sasa_normal(pose, probe_size=1.1):
21     sasas = rosetta.core.id.AtomID_Map_double_t()
22     rsd_sasa = rosetta.utility.vector1_double()
23     rosetta.core.scoring.calc_per_atom_sasa(pose, sasas, rsd_sasa, probe_size, False
24     )
25     return sasas
26
27 pdbbs = []
28
29 with open('short_pdbbs.csv', 'r') as file:
30     pdbbs = [pdb.rstrip() for pdb in file.readlines()]
31
32 start = time.time()
33 for pdb in pdbbs:
34
35     pose = pose_from_file(pdb)
36
37     dalstart = time.time()
38     surf_vol = get_per_atom_sasa_dalpha_ball(pose)
39
40     dal = 0
41
42     for i in range(1, pose.size()+1):
43         res = pose.residue(i)
44         for j in range(1, res.natoms()+1):
45             dal += surf_vol.surf(i, j)
46
47     dalend = time.time()
48
49     df = df.append(pd.Series([pdb, 'Power Method', dal], index=df.columns),
50     ignore_index=True)
51     daltimes = daltimes.append(pd.Series([pdb, pose.size(), dalend - dalstart],
52     index=daltimes.columns), ignore_index=True)
53
54 mid = time.time()
55 for pdb in pdbbs:
56
57     pose = pose_from_file(pdb)
58
59     voxstart = time.time()
60     normal_sasa = get_per_atom_sasa_normal(pose)
61
62     sasa = 0
63     for i in range(1, pose.size()+1):
64         res = pose.residue(i)
65         for j in range(1, res.natoms()+1):
66             sasa += normal_sasa(i, j)
67
68     voxend = time.time()

```

```

68     df = df.append(pd.Series([pdb, 'Shrake-Rupley', sasa], index=df.columns),
69                     ignore_index=True)
70     voxtimes = voxtimes.append(pd.Series([pdb, pose.size(), voxend - voxstart],
71                                         index=voxtimes.columns), ignore_index=True)
72
73 end = time.time()
74
75 times = open('times.txt', 'w')
76 times.write("Power Method Time: {}\n".format(mid - start))
77 times.write("Shrake-Rupley Time: {}\n".format(end - mid))
78 times.close()
79
80 df.to_csv('values.csv', index=False, header=False)
81 daltimes.to_csv('daltimes.csv', index=False, header=False)
82 voxtimes.to_csv('voxtimes.csv', index=False, header=False)
83
84 print("Power Method Time: {}".format(mid - start))
85 print("Shrake-Rupley Time: {}".format(end - mid))
86
87 fig, axes = plt.subplots(nrows=1, ncols=2, sharex=True, sharey=True)
88
89 # drop sharex, sharey, layout & add ax=axes
90 df.hist(column='sasa', by='type', ax=axes)
91
92 # set title and axis labels
93 plt.suptitle('Computing SASA: Power Method vs. Shrake-Rupley', x=0.5, y=1.00, ha='
94               center', fontsize='large')
95 fig.text(0.5, 0.02, 'Calculated SASA', ha='center')
96 fig.text(0.01, 0.5, 'Number of Structures', va='center', rotation='vertical')
97
98 plt.savefig('sasa.png')
99
100 fig2 = daltimes.plot.scatter(x='Residue Count', y='Time (s)')
101 plt.title("Power Method Time vs. Residue Count")
102 plt.savefig('daltimes.png')
103
104 fig3 = voxtimes.plot.scatter(x='Residue Count', y='Time (s)')
105 plt.title("Shrake-Rupley Time vs. Residue Count")
106 plt.savefig('voxtimes.png')

```

8 References

- [1] Bryant, R, Edelsbrunner, H, Koehl, P, Levitt, M. The Area Derivative of a Space-Filling Diagram. *Discrete & Computational Geometry*. 32 (2004), 293-308.
- [2] DeCoste, Donald J, Zumdahl, Steven S. *General Chemistry 142* University of Washington 7th Edition, Boston, Cengage Learning, 2015.
- [3] Edelsbrunner, H. The Union of Balls and Its Dual Shape. *Discrete & Computational Geometry*. 13 (1995), 415-440.
- [4] Fischer, Kaspar. *Introduction to Alpha Shapes*. Stanford University, lecture notes, 2011.

- [5] Le Grand, Scott M., Merz, Kenneth M. Jr. Rapid approximation to molecular surface area via the use of Boolean logic and look-up tables. *Journal of Computational Chemistry*. 14 (1993). 349-352.
- [6] H.M. Berman, J. Westbrook, Z. Feng, G. Gilliland, T.N. Bhat, H. Weissig, I.N. Shindyalov, P.E. Bourne. (2000) *The Protein Data Bank Nucleic Acids Research*, 28: 235-242.
- [7] Richmond, Timothy J. Solvent Accessible Surface Area and Excluded Volume in Proteins. *J. Mol. Biol.* 178 (1984), 63-89.
- [8] Rotskoff, Grant. The Gauss-Bonnet Theorem. University of Chicago REU, paper, 2010
- [9] S. Chaudhury, S. Lyskov & J. J. Gray, "PyRosetta: a script-based interface for implementing molecular modeling algorithms using Rosetta," *Bioinformatics*, 26(5), 689-691 (2010).
- [10] Schnell, Christian. The Gauss-Bonnet Theorem. talk at Columbus, 2004.

List of Figures

1	Calculation of d_{iq} and θ_{iq} for the purpose of calculating m_{iq} .	4
2	Two Intersecting Spheres	5
3	B_1 is bound by a sphere. The radius of the solvent is the distance between the edge of the ball and the sphere.	6
4	Three balls in space bounded by three different spheres. Their centers are used for Delaunay Triangulation.	7
5	A power diagram comprised of power cells (left) and its Delaunay Triangulation (right).[1]	7
6	The dual complex (K) of the Delaunay Triangulation only includes those power cells that have a non-empty intersection.[1]	7
7	The star of K and link of the star are shown.[1]	8
8	Two intersecting spheres S_i and S_j . [1]	10
9	Three intersecting spheres at two points: S_i , S_k and S_j . [1]	12
10	Plot of Computation Time versus Residue Count (Power Method)	15
11	Plot of Computation Time versus Residue Count (Shrake-Rupley Method)	15
12	SASA Histograms for the Two Algorithms	16